Available online at www.sciencedirect.com
ScienceDirect
Journal of Photochemistry and Photobiology A: Chemistry 195 (2008) 368–377
Journal of Photochemistry and Photobiology A:Chemistry
www.elsevier.com/locate/jphotochem

Photophysical characterization and effect of pH on the twisted intramolecular charge transfer fluorescence of *trans*-2-[4-(dimethylamino)styryl]benzothiazole

Subit Kumar Saha [a,*], Pradipta Purkayastha [a,*], Asim Bikas Das [b]

[a] *Chemistry Group, Birla Institute of Technology and Science, Pilani 333031, Rajasthan, India*
[b] *Biological Sciences Group, Birla Institute of Technology and Science, Pilani 333031, Rajasthan, India*

Received 3 August 2007; received in revised form 11 October 2007; accepted 2 November 2007
Available online 17 November 2007

Abstract

Experimental and theoretical photophysical characterization of *trans*-2-[4-(dimethylamino)styryl]benzothiazole (DMASBT) has been carried out in solutions of different polarities. Steady state fluorescence emission and excitation spectra of DMASBT in the solvents of varying polarities suggest the existence of dual emitting states where locally excited state is responsible for fluorescence in nonpolar solvents; however, in polar solvents fluorescence is from twisted intramolecular charge transfer (TICT) state. Solvatochromic comparison method suggests that the dipolar interactions make the major contribution to the stability of ground as well as excited states with more effect on the latter. Semi-empirical AM1 singly excited configuration interaction (AM1-SCI) calculations support the formation of the TICT state of DMASBT. The twist of the $-N(CH_3)_2$ group and the change in its hybridization in the excited state develops a high dipole moment in the S_3 state and thereby stabilizing it to give the TICT fluorescence in polar solvents. The TICT fluorescence of DMASBT decreases above the pH value of 3.7 suggesting that hydrogen bonding ability of water molecules becomes efficient above this pH. Results indicate that DMASBT can be a potential sensor based on its remarkably high fluorescence sensitivity towards polarity, viscosity and pH of the medium.

Keywords: Fluorescence; Styrylbenzothiazole; Twisted intramolecular charge transfer; Polarity; Acidity constant; AM1-SCI

1. Introduction

Intermolecular and intramolecular electron donor–acceptor systems that explain the charge transfer phenomenon has been a topic of interest to many from long back [1–4]. The concept of intramolecular charge transfer originated quite a few decades ago and is still carrying a lot of interest and opening grounds for important inventions regarding the characterization of relevant molecules where the long wavelength, low-energy, structureless charge transfer band is the principal feature [5,6]. Highly Stokes shifted fluorescence band of such molecules, which develops as a result of twisting of the donor part around the single bond connecting the donor to the acceptor system, is known as the fluorescence due to twisted intramolecular charge transfer (TICT) according to Rotkiewicz and Grabowski in their pioneering works with *p*-(*N*,*N*-dimethylamino)benzonitrile (DMABN) in polar solvents [7,8]. The idea of the TICT state is based on a principle that associates minimum orbital overlap with intramolecular charge separation [8,9]. In this context, a recent work of Cuquerella et al. [10] can be mentioned where they explained the photophysics of Norfloxacin and its derivatives exploiting the TICT phenomenon in the molecule. Their study reveals that the geometry of fluoroquinolone main system changes from an almost piperazinyl pyramid in the ground state to nearly trigonal planar in the excited singlet state due to a change in the hybridization of the nitrogen atom. Apart from this, recently Druzhinin et al. [11] demonstrated an ultrafast intramolecular charge transfer (ICT) in DMABN, where they have taken acetonitrile as the solvent medium. The essential difference between the TICT and the other ICT models for molecules such as DMABN is

* Corresponding authors. Tel.: +91 1596 245073x238; fax: +91 1596 244183.
E-mail addresses: sksaha@bits-pilani.ac.in, subitk_saha@yahoo.com (S.K. Saha), ppurkayastha@bits-pilani.ac.in (P. Purkayastha).

1010-6030/$ – see front matter © 2007 Elsevier B.V. All rights reserved.
doi:10.1016/j.jphotochem.2007.11.004

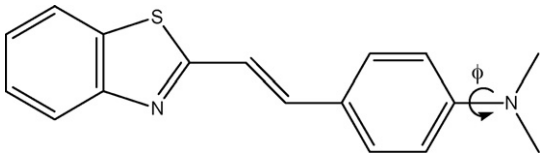

Scheme 1. *Trans*-2-[4-(dimethylamino)styryl]benzothiazole (DMASBT).

the absence of electronic coupling between the amino and benzonitrile groups in the TICT state (principle of zero electronic overlap) [12,13].

A recent report of Fayed and Ali demonstrates the protonation dependent intramolecular charge transfer in 2-[4-(dimethylamino)styryl]benzazoles, where they have compared the ICT properties of 2-[4-(dimethylamino)styryl]benzoxazole (DMASBO) with that of 2-[4-(dimethylamino)styryl]-benzothiazole (DMASBT) [14]. Unfortunately, they have explained the ICT to be because of the increase in the dipole moment of the S_1 state. They could not identify the stability of the S_3 state as the responsible factor that thereby produces the TICT fluorescence. Moreover, they have not considered the twist of the $–N(CH_3)_2$ at all, which is, in fact, the most important factor of the process. The stability of the S_3 state is achieved because of the development of a very high dipole moment of the molecule in the excited state at a twist angle of 90° of the $–N(CH_3)_2$ group accompanied by a change in the shape of the group because of a change in the hybridization of the nitrogen atom. The study of Fayed and Ali needs thorough revision since TICT in DMASBT can make the compound a very sensitive candidate as a biosensor. Principally driven by the medical importance of *trans*-2-[4-(dimethylamino) styryl]benzothiazole (Scheme 1) we thought about its thorough characterization. Dey et al. [15] have reported the dual fluorescence of 2-(4-(*N*,*N*-dimethylamino)phenylbenzothiazole (DMAPBT) molecule. DMASBT is different from DMAPBT by a double bond incorporated between a benzothiazole ring and a *N*,*N*-dimethylaminophenyl ring in such a way that these two rings are at *trans* position with respect to the double bond.

There are reports on the effect of solvent polarity and viscosity on TICT properties of various molecular systems such as coumarins, DMABN, a group of molecules called molecular rotors, etc. [16,17]. Although solvent polarity causes a bathochromic shift of the emission band in all these compounds, this shift is smallest in the case of molecular rotors. Peak intensity is influenced strongly by solvent viscosity in DMABN and the molecular rotors but polarity and viscosity influences cannot be separated with DMABN. Coumarins, on the other hand are not sensitive to viscosity. Interestingly in DMASBT both solvent polarity and viscosity have their own effects on emission intensity as well as on emission wavelength unlike coumarins and molecular rotors. As mentioned above, DMASBT can be a very potential candidate as sensitive biosensor because of its structural nature. Experimental findings indicate the sensibility of DMASBT under different environmental conditions and quantum chemical AM1-SCI calculations have rationalized the experimental data.

2. Experimental

2.1. Materials and methods

DMASBT was procured from Aldrich Chemical Company, WI, USA and was recrystallized from a mixture of ethanol and a small percentage (∼10%) of *n*-hexane. A single spot was noticed for the recrystallized compound in thin layer chromatography (TLC) plate. All the solvents used are of spectroscopic grade and procured from Spectrochem Chemical Company, India. Triple distilled water was used for the preparation of the aqueous solutions. Dilute sulfuric acid and sodium hydroxide solutions were used to adjust the pH of the prepared solutions. A stock solution of DMASBT (1.001×10^{-3} M) was prepared in pure methanol to record the UV–vis absorption and fluorescence spectra of DMASBT in pure solvents; 0.1 mL of this solution was poured in a 10 mL volumetric flask and left for a few hours for complete evaporation of methanol and then the compound was dissolved in respective solvents to make the final volume to 10 mL. To prepare the solutions of the compound in dioxane–water mixtures, 0.1 mL of dioxane solution of DMASBT (1.001×10^{-3} M) was pipetted out and poured into a 10 mL volumetric flask, and the final volume of the solution was made to 10 mL with required amount of dioxane and water. The concentration of DMASBT in all the experimental solutions used for spectroscopic measurements was 1.001×10^{-5} M. The fluorescence quantum yields were determined with respect to that of quinine sulfate in 0.1N H_2SO_4 (0.55). The absorption spectra were recorded using a Jasco V570 UV–vis spectrophotometer. Fluorescence measurements were performed using a Shimadzu RF-5301PC scanning spectrofluorimeter. ELICO LI610 pH meter was used to measure the pH of the solutions.

2.1.1. Solvatochromic comparison method (SCM)

To find the information about the individual contribution of different solvent effects a multiparametric approach, known as solvatochromic comparison method proposed by Kamlet et al. [18], has been used. This approach separates the dielectric effects of solvents (π^*), hydrogen-bond donor ability (α), and hydrogen-bond acceptor ability (β) of the solvents on the spectral properties. The equation describing these effects is:

$$E = E^0 + c\pi^* + a\alpha + b\beta \quad (1)$$

where, a, b, and c are the coefficients and E^0 is the spectral maxima independent of solvent effects. The values of π^*, α, and β of different solvents have been taken from the report of Kamlet et al. [18]. The values of E are absorption/fluorescence band maxima in terms of cm^{-1}.

2.1.2. Calculation of excited state acidity constant (pK_a^*)

pK_a^* has been calculated by fluorometric titration method [19–21]. In this method, the relative fluorescence intensities (I/I_0) at a particular wavelength of acid and its conjugate base are plotted separately against pH. These sigmoid curves intersect at a point ($I/I_0 = 0.5$) if these are the only two species present, and that pH value represents the pK_a^*.

2.1.3. Quantum chemical calculations

Hyperchem package Version 6.01 (Hypercube Inc., Canada) has been used for the theoretical calculations. The ground state (S_0 geometry) of the compound was optimized by AM1 method [22,23]. AM1-SCI (singly excited configuration interaction) was performed to get the energy (E_g) and dipole moment in the ground state and the transition energies ($\Delta E_{i\rightarrow j}$), and dipole moments of different excited states. We have taken care of all the singly excited configurations within an energy window of 11 eV from the ground state. $\Delta E_{i\rightarrow j}$ corresponds to the excitation of an electron from the orbital ϕ_i (occupied in the ground state) to the orbital ϕ_j (unoccupied in the excited state). The total energy of the excited state (E_j) was then calculated as $E_j = E_g + \Delta E_{i\rightarrow j}$. The CI wavefunction has been used to generate g orbitals and one-electron density matrices, which were used to calculate the dipole moments of the excited states of the compounds. The stabilization of the different states due to solvation has been calculated from the solvation energies based on Onsager's theory [24]. Assuming that the solute molecule having a dipole μ_i in the ith electronic state is fully solvated, the solvation energy is given by,

$$\Delta E_{solv} = \frac{2\mu_i^2(\varepsilon - 1)}{a^3(2\varepsilon + 1)} \quad (2)$$

where ε is the relative permittivity of the solvent and a is the cavity radius.

3. Results and discussion

3.1. UV–vis absorption study of DMASBT

The UV–vis absorption spectra of DMASBT in pure solvents of different polarities show the normal trend of red shift of the long wavelength absorption band maximum (λ_{max}^{ab}) with increasing polarity of the solvents (Table 1). The structured character of the absorption bands observed in nonpolar and/or less polar solvents progressively diminishes with increasing polarity of the solvent media, which suggests some sort of interaction between DMASBT and the polar solvent molecules [25,26]. In agreement with the arguments given by Mallick et al. [25] about their study on steady state photophysics of a quinolizine derivative, we also state that the ground state charge transfer character of DMASBT is absent in polar solvents. The absorption data have been analyzed using the solvent comparison method proposed by Kamlet et al. [18]. The equation obtained from this approach with regression coefficient value 0.92 is as follows:

$$E\,(\mathrm{cm}^{-1}) = 26048 - 807.2\pi^* + 100.94\alpha - 88.95\beta \quad (3)$$

The negative values of 'c' and 'b' indicate stabilization, whereas positive value of 'a' indicates destabilization. The positive value of 'a' is consistent with the fact that donation of lone pair of electrons of the nitrogen atom of $-N(CH_3)_2$ group to hydrogen bonding solvent hinders the participation of the lone pair with the π-cloud of the ring and thus destabilizing the system. However, the observed red shift of absorption maxima with increasing the solvent polarity indicates that the dipolar interactions offer major contribution. Therefore, highly red-shifted structureless bands observed in polar solvents like water, acetonitrile, DMF and DMSO are mainly due to the presence of dipole–dipole interactions.

3.2. Fluorescence study of DMASBT

The emission spectra of DMASBT in some of the pure solvents of different polarities are shown in Fig. 1. Similar to the

Table 1
Absorption wavelength maxima [λ_{max}^{ab} (nm)], log $\in_{max}$, fluorescence wavelength maxima [λ_{max}^{fl} (nm)][a], fluorescence quantum yields (φ_f) and Stokes shift (ν_{ss}) of DMASBT in different solvents along with their $E_T(30)$ (kcal mol^{-1}) values

Solvents	$E_T(30)$	λ_{max}^{ab} (nm)	log $\in_{max}$[b]	λ_{max}^{fl} (nm)	ν_{ss} (cm^{-1})	φ_f (±0.0001)[c]
Cyclohexane	30.9	384	4.44	447	3671	0.0010
Heptane	31.1	387	4.45	446	3418	0.0014
Hexane	32.4	384	4.53	445	3604	0.0018
Diethyl ether	34.5	390	4.48	460	3902	0.0020
1,4-Dioxane	36.0	393	4.36	467	4032	0.0022
THF[d]	37.4	396	4.57	482	4506	0.0030
Ethylacetate	38.1	391	4.29	477	4611	0.0053
DMF[e]	43.6	402	4.41	504	5035	0.0070
DMSO[f]	44.8	405	4.36	513	5198	0.0078
Acetonitrile	45.6	401	4.35	504	5097	0.0066
Isopropanol	48.4	394	4.23	493	5097	0.0048
Ethanol	51.9	396	4.29	498	5173	0.0045
Methanol	55.4	397	4.28	507	5465	0.0030
Glycerol	56.7	409	4.25	530	5582	0.1150
Water[g]	63.1	402	4.10	516	5496	0.0012

[a] λ_{ex} = 395 nm.
[b] [DMSBT] = 1.001 × 10^{-5} M.
[c] Fluorescence quantum yields at λ_{ex} = 395 nm.
[d] Tetrahydrofuran.
[e] Dimethylformamide.
[f] Dimethylsulfoxide.
[g] pH of aqueous solution is 7.2.

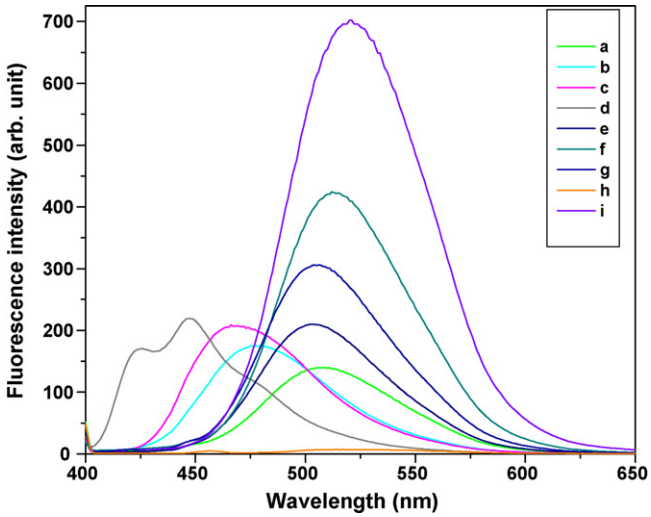

Fig. 1. Fluorescence spectra of DMASBT in different pure solvents at [DMASBT] = 1.001 × 10^{-5} M and λ_{ex} = 395 nm; (a) methanol, (b) ethylacetate, (c) dioxane, (d) cyclohexane, (e) acetonitrile, (f) DMSO, (g) DMF, (h) water, and (i) glycerol.

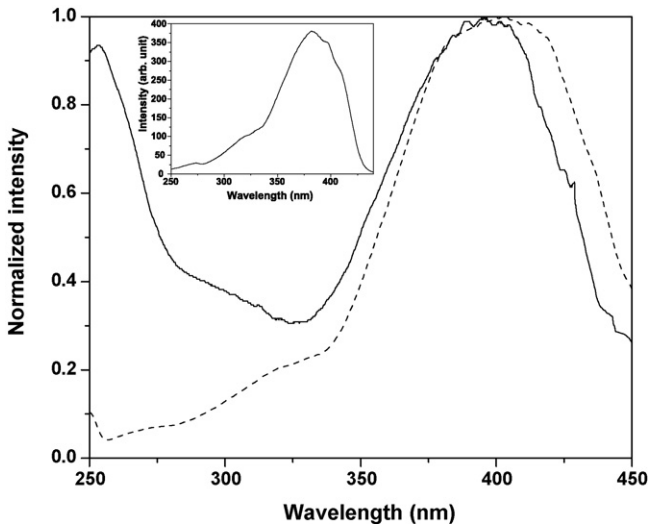

Fig. 2. Normalized absorption (—) and excitation (- - -) spectrum (λ_{em} = 500 nm) of DMASBT in methanol. Inset: excitation spectrum of DMASBT in cyclohexane (λ_{em} = 500 nm).

absorption bands, the emission bands are also structured in nonpolar solvents and have mirror image relationship with their respective absorption spectra. This confirms that there is no change in geometries between absorbing and emitting species in a nonpolar solvent. Appearance of a broad red-shifted fluorescence band with gradual disappearance of vibrational structures with increasing solvent polarity indicates the development of the charge transferred (CT) state in a polar solvent [25]. The fluorescence band maxima (λ^{fl}_{max}) are listed in Table 1. Emissions in nonpolar solvents can be ascribed to originate from the locally excited (LE) state. Upon excitation, transfer of an electronic charge occurs from a donor (D) to an acceptor (A) site leading to a charge separation. This process is called as twisted intramolecular charge transfer proposed by Grabowski et al. [8,27] and the resulting state is labeled as TICT state which is believed to be responsible for the anomalous fluorescence. In this process, a positive and a negative charge are localized in two different and separated functional parts of the molecule resulting in an increase in the molecular dipole moment. Contrary to DMABN, DMASBT does not exhibit dual emission peaks like coumarins [((7-amino-4-methylcoumarin-3-acetyl)amino)hexanoic acid, coumarin 1, and coumarin 6] [16].

Fluorescence excitation spectra have been recorded in solvents of varying polarities to establish that the fluorescence of DMASBT are from two different emitting states (LE and TICT) although there is a single absorbed species. Fig. 2 represents the absorption and excitation spectra (λ_{em} = 500 nm) of DMASBT in methanol. The band maximum of the latter differs by 7 nm from that of the absorption spectrum indicating that the absorbed and emitted species are different. The spectrum in the inset is the excitation spectrum of DMASBT (λ_{em} = 500 nm) in cyclohexane. The band maximum, in this case, is same as that of absorption spectrum (384 nm) with structured characteristics of band. Therefore, it can be concluded that emissions in nonpolar solvents originate only from the LE state where the absorbed species is same as the emitted species. However, emission in a polar solvent is mainly from a state, which is created at the excited state assigned as charge transfer state.

Calculated values of fluorescence quantum yields and Stokes shifts are also listed in Table 1. It can be seen that fluorescence quantum yield increases and then decreases with increasing $E_T(30)$, an empirical solvent polarity parameter [28,29], which includes the effects of specific as well as non-specific interactions. However, the disadvantages of such scales are that the information about the individual contribution of different solvent effects is lost. The data in Table 1 show that the Stokes shift increases with increasing the $E_T(30)$ of pure solvents.

SCM has also been applied to analyze the fluorescence data, which results into the following equation with regression coefficient value = 0.96:

$$E\,(\mathrm{cm}^{-1}) = 22468.43 - 2052.49\pi^* - 368.45\alpha - 379.16\beta \quad (4)$$

This equation shows that all the three parameters, π^*, α, and β, contribute to the stabilization of excited state. Compared to ground state, negative value of '*a*' indicates that the stabilization is also due to hydrogen-bond donor ability of solvents. This favors that although the lone pair of electrons on the N-atom of $-N(CH_3)_2$ group is not available due to their involvement in the formation of the charge transfer state, but that on the tertiary N-atom of the benzothiazole moiety is available for donation to the hydrogen bonding solvents. This, in turn, favors the stability of the excited state. Eq. (4) shows that greater contribution to the stability of the excited state is also due to dipole–dipole interactions like ground state stabilization. But, this contribution is greater in the excited state than that in the ground state, which also supports that the excited state dipole moment of DMASBT (see later) is greater than the ground state dipole moment. This explanation supports the high Stokes shift values in polar solvents. In the cases of

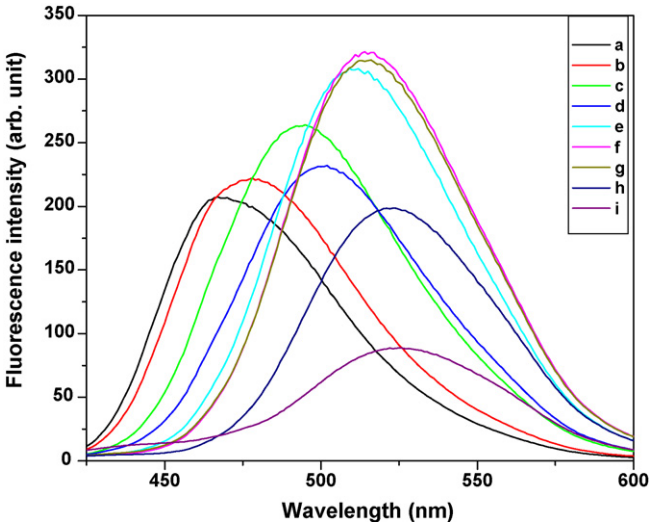

Fig. 3. Fluorescence spectra of DMASBT in different percentages of dioxane in water; (a) 100, (b) 98, (c) 90, (d) 80, (e) 60, (f) 50, (g) 40, (h) 30, and (i) 20. λ_{ex} = 408 nm, [DMASBT] = 1.001 × 10^{-5} M. Only a few of the spectra have been shown for clarity. Fig. 4 contains the Stokes shift values for all the spectra taken for different water concentrations in dioxane.

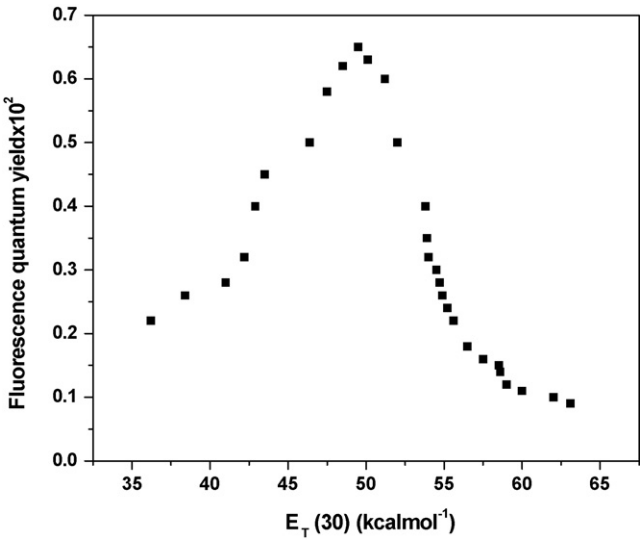

Fig. 5. Plot of variation of fluorescence quantum yields against $E_T(30)$ of dioxane–water mixture. λ_{ex} = 408 nm, [DMASBT] = 1.001 × 10^{-5} M.

DMF, DMSO and glycerol high fluorescence quantum yields are observed. This is probably due to the higher viscosity of these solvents compared to other solvents thus restricting a degree of nonradiative processes as observed by Dey et al. [15] in 9-(*N*,*N*-dimethylamino)anthracene (9-DMA) and by Haidekker et al. [16] in DMABN and 9-(dicyanovinyl)-julolidine (DCVJ).

The fluorescence spectra of DMASBT in different percentages of dioxane in water are shown in Fig. 3. The fluorescence band gets red shifted with increasing percentage of water in the mixture. Fig. 4 and its inset show the variations of Stokes shift (ν_{ss}) and energy corresponding to fluorescence maxima (E_f), respectively, whereas Fig. 5 depicts fluorescence quantum yields

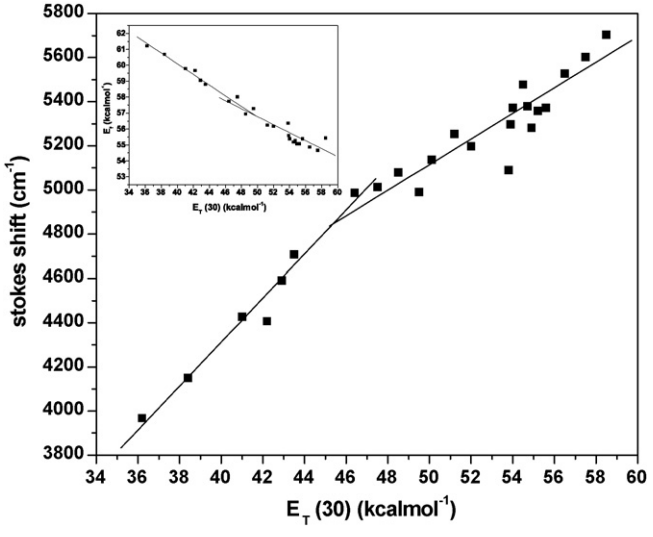

Fig. 4. Plot of variation of Stokes shift of DMASBT against $E_T(30)$ of dioxane–water mixture. Inset: variation of energy corresponding to fluorescence maxima (E_f) against $E_T(30)$ of dioxane–water mixture.

(ϕ_{fl}) of DMASBT with increasing the $E_T(30)$ of dioxane–water mixtures. Fig. 4 shows a linear variation of Stokes shift up to a certain value of $E_T(30)$. At this point it can be stated that the stabilization of the ICT state is very sensitive to the change in polarity of the medium up to a certain extent, after that the sensitivity towards polarity decreases may be due to the fact that the extent of stabilization due to specific interactions (hydrogen bonding) becomes progressively less important with increasing the concentration of water in dioxane–water mixture. This can be supported by the nature of the plot in inset of Fig. 4, in which it is observed that the initial decrease of energy corresponding to fluorescence maxima (E_f) is greater than that in the higher polarity region quite in contrast to that observed by Mallick et al. in case of a quinolizine derivative showing ICT fluorescence [25]. When plotted against the $E_T(30)$ values of the mixed solvents, the fluorescence quantum yield shows an initial hike up to a certain magnitude of polarity followed by a concomitant decrease with further increase in the polarity of the environment (Fig. 5). In nonpolar solvent, like dioxane, emission takes place from the LE state; with increasing concentration of water, due to the increase in polarity of the solvent, the more polar ICT state gets progressively stabilized resulting into a red shift of the emission band maximum and an increase in fluorescence quantum yield. After a certain critical concentration of water (∼50%) in the mixture, the ICT state gets further stabilized due to solvation and comes closer to the nearby triplet state as well as to the ground state, which leads to enhancement of the rate of nonradiative processes (*viz.*, internal conversion (IC), and intersystem crossing (ISC)). For example, in pure water the solvated S_3 energy is −3860.73 kcal mol^{-1} and that of the corresponding solvated T_{12} state is −3860.56 kcal mol^{-1} indicates the proximity that is required for ISC to occur efficiently.

Ravi et al. [30] reported a very effective method to determine the difference between the dipole moments of the excited and the ground states ($\Delta\mu$). To obtain this value, Stokes shifts can be

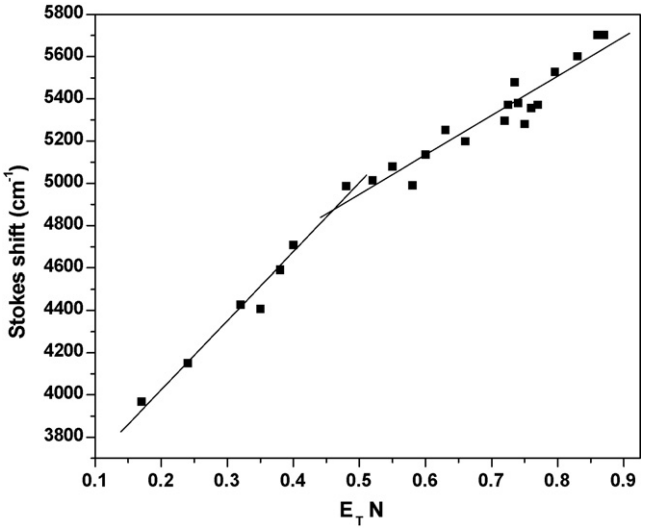

Fig. 6. Plot of variation of Stokes shift against E_T^N of dioxane–water mixtures.

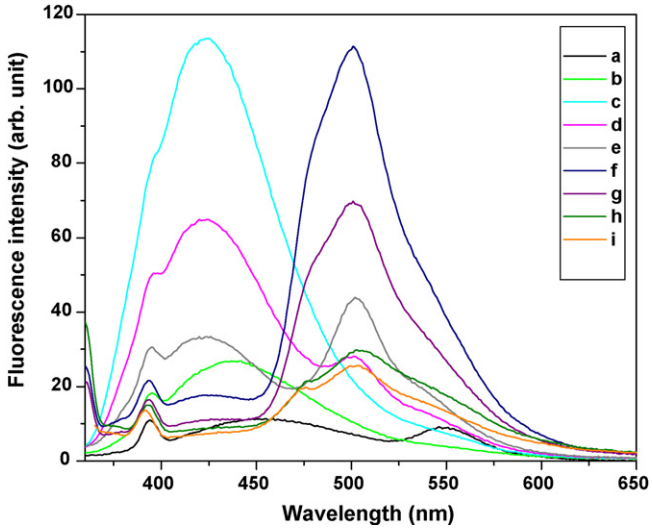

Fig. 7. Fluorescence spectra of DMASBT in aqueous solution of different pH; (a) 0.27, (b) 0.92, (c) 1.88, (d) 2.38, (e) 2.65, (f) 3.7, (g) 4.01, (h) 5.58, and (i) 6.98. λ_{ex} = 345 nm, [DMASBT] = 1.001×10^{-5} M.

plotted against E_T^N of dioxane–water mixtures (Fig. 6) according to Eq. (5)

$$\text{Stokes shift}\,(\text{cm}^{-1}) = 11307.6\left\{\left(\frac{\Delta\mu}{\Delta\mu_D}\right)^2\left(\frac{a_D}{a}\right)^3\right\}E_T^N + Y^*(m, g) \quad (5)$$

where $\Delta\mu_D$ = 9 D, the change in dipole moment on excitation of pyridinium *N*-phenoxide betaine dye, a_D = 6.2 Å is its Onsager cavity radius [30], *a* is radius of molecule of interest and $Y^*(m,g)$ is a constant. Similar to Fig. 4, Fig. 6 also shows the deviation from linear relationship between Stokes shift and E_T^N of dioxane–water mixtures at a higher percentage of water in the overall mixture. $\Delta\mu$ calculated from the slope of the first segmented linear portion of Fig. 6 is found to be 8.06 D. The Onsager's cavity radius (*a*) of DMASBT is taken to be 7.79 Å (obtained from the calculation using AM1 method). Using the calculated ground state dipole moment value of DMASBT i.e., 3.20 D, the dipole moment of the excited state CT species comes out to be 11.26 D. Theoretical calculations (discussed later) show that the S_3 state is responsible for the polarity induced TICT emission. The calculated value of dipole moment of the S_3^{TICT} state (12.5 D) is in well agreement with the experimental value (11.26 D). Since the dipole moment of this S_3^{TICT} state (μ = 12.5 D) is much greater than that of the ground singlet TICT state (S_0^{TICT}, μ = 0.8 D), the former is much more polar. Therefore, S_3^{TICT} state becomes relatively more stabilized as compared to the S_0^{TICT} state by the influence of the polar medium. This results into a decrease in the energy gap, ΔE ($S_3^{TICT} - S_0^{TICT}$), with a consequent red shift in the TICT emission. As a result of that the rate of internal conversion from S_3^{TICT} to S_0^{TICT} is higher in water than that in less polar solvents. This fact is in favor of the stronger TICT emission in the less polar medium as compared to that in pure water [25]. Moreover, TICT emissions in less polar solvents are also increased due the decrease in the rate of intersystem crossing from the S_3^{TICT} state to triplet TICT state [31]. Hydrogen-bonding interaction between DMASBT and water is also responsible for fluorescence quenching [32,33] due to radiationless transitions, e.g., in the cases of some dyes, stronger hydrogen-bonding solvents have been found to enhance the rate of singlet-triplet intersystem crossing [34]. As a result of that, a weak TICT emission of DMASBT is observed in pure water.

3.3. Effect of hydrogen ion concentration on absorption and fluorescence spectra

The absorption spectrum of DMASBT taken at pH 0.27 exhibits two bands, one is red shifted (λ_{max}^{ab} = 455 nm) and the other is blue shifted (λ_{max}^{ab} = 351 nm) with respect to the long wavelength absorption band (λ_{max}^{ab} = 415 nm) of the neutral DMASBT molecule. The fluorescence spectra at different pH values are shown in Fig. 7. The fluorescence spectra obtained by exciting DMASBT at the respective band maxima of the above mentioned two absorption bands are also different and similar to the absorption spectrum; one of them is red shifted (λ_{max}^{fl} = 549 nm) and the other is blue shifted (λ_{max}^{fl} = 456 nm) with respect to that of the neutral molecule (λ_{max}^{fl} = 508 nm). In this case, the lower value of λ_{max}^{fl} (508 nm) for the neutral molecule compared to that in pure water (λ_{max}^{fl} = 516 nm) is due to the presence of 1% methanol as a cosolvent, most probably because of the exceptional sensitivity of DMASBT towards polarity. In addition to that, the fluorescence excitation spectrum corresponding to the blue-shifted fluorescence band matches exactly with the short wavelength absorption band while that for the red-shifted fluorescence band resembles the long wavelength absorption band. This suggests the formation of two different kinds of monocation species. The red-shifted absorption or emission band corresponds to the monocation I (Scheme 2), formed due to the addition of proton to the heterocyclic nitrogen of the benzothiazole ring and the blue-shifted absorption or emission band is associated with the monocation II formed as a result of protonation at the dimethylamino nitrogen. Since the lowest energy transition of the molecule is $\pi \rightarrow \pi^*$ in nature, the proto-

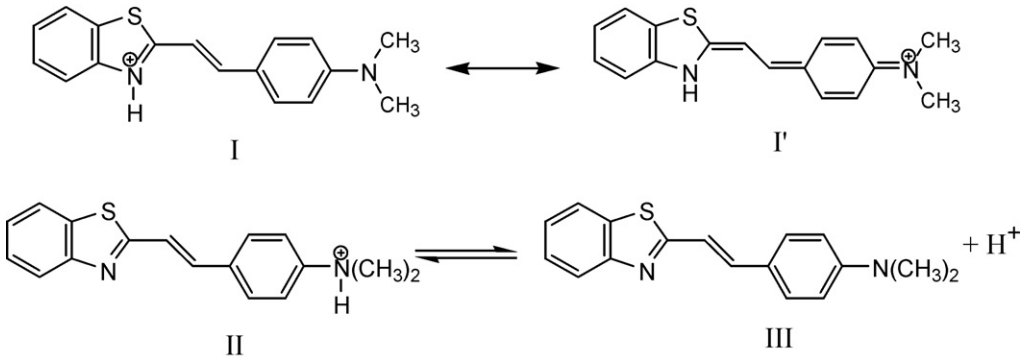

Scheme 2. Behavior of DMASBT in different pHs of the aqueous medium.

nation at the heterocyclic nitrogen atom will shift the absorption and fluorescence band to the red, whereas the same at the nitrogen atom of $–N(CH_3)_2$ group will shift the band to the blue with respect to that of the neutral molecule. The large red shift for the monocation I, can be explained by the resonance interaction of the $–N(CH_3)_2$ group with the styrylbenzothiazole part of the molecule that leads to structure I′ responsible for the stabilization of the species. The formation of both types of monocations (monocations I and II) indicates the involvement of the lone pair of electrons of $–N(CH_3)_2$ group in resonance interaction, thus reducing the charge density on the nitrogen atom of $–N(CH_3)_2$ group and enhancing the same on the heterocyclic nitrogen atom. Therefore, protonations at both types of nitrogen atoms are possible at lower pH as observed in case of DMAPBT molecule reported by Dey et al. [15].

As the pH of the medium increases the intensity of the fluorescence band corresponding to species I decreases whereas that of the species II increases and reaches the maximum value at pH 1.88. It appears that with decreasing the concentration of hydrogen ions the possibility of formation of monocation I is reduced. Above pH 1.88, the intensity of the monocation II starts decreasing and at the expense of that a new band starts appearing in the wavelength region lying between the above mentioned two bands; the λ^{fl}_{max} for this new band is equal to 508 nm, which is almost same as λ^{fl}_{max} of TICT band in water. The appearance of TICT emission band of DMASBT at pH 2.38 is shown in Fig. 7, intensity of which becomes maximum at pH ∼ 3.7. All these observations indicate an equilibrium between monocation II and the neutral DMASBT in the pH range of 1.88–3.7. The pK^* (excited state protonation constant) of this equilibrium, calculated by fluorimetric titration method [19–21] is found to be 2.77. The monocation II shows its maximum accumulation at a pH of 1.88. With increasing pH the equilibrium concentration of the neutral species (i.e. species III in Scheme 2) increases in the equilibrium between species II and III. This results in an increase in fluorescence intensity of species III. It can be seen in Fig. 7 that when intensity of species II at pH 3.7 is very low, the intensity of species III becomes close to the intensity of species II at pH 1.88. The pK^*_a of this equilibrium is found to be 2.77, whereas the ground state protonation constant (pK_a) of the same equilibrium comes out to be 4.8. The higher value of pK_a compared to pK^*_a can be explained by the fact that basicity of N-atom of $–N(CH_3)_2$ decreases due to a greater extent of charge transfer from the same N-atom on excitation that results in the lowering of equilibrium concentration of species II in the excited state [21,34]. The appearance of a new band at pH 2.38 suggests that this band is due to the TICT emission, which is the only predominant emission that can exist in water. This also confirms that monocation II is formed as a result of protonation of N atom of $–N(CH_3)_2$ group, for which TICT band is not expected due to the engagement of lone pair of electrons with the H^+ ion. It is worth mentioning here that no TICT band appears at pH 0.27 for monocation I, although it involves greater charge transfer from N-atom of $–N(CH_3)_2$ group to the protonated benzothiazole ring. The protonation of N-atom in this ring facilitates the conjugation of the $–N(CH_3)_2$ group with the π-system of DMASBT, which in turn leads to the appearance of a double bond character of the phenyl carbon–nitrogen bond (resonating structure I′ in Scheme 2) and thus reducing the rotational relaxation of the $–N(CH_3)_2$ group in the excited singlet state.

The TICT fluorescence intensity of DMASBT reaches its maximum value at pH ∼ 3.7 after which the fluorescence intensity starts decreasing and becomes constant at a pH ∼ 7. Therefore, from this observation it can be concluded that the H-bonding effect of water becomes important only when the pH of the solution is greater than 3.7. Increasing the pH of the solution above 3.7 drives more and more H_3O^+ ions to loose a proton to form H_2O. As a consequence the efficiency of H-bonding interactions increases, thus decreasing the TICT fluorescence intensity, which attains its minimum constant value at around pH 7. This observation indicates the sensing efficiency of DMASBT towards H-bonding interaction. Fayed and Ali [14] have also studied the effect of acid concentration on the spectral behavior of DMASBT. However, in the present study pK_a, and pK^*_a values of monocation II-neutral species equilibrium have been calculated and compared. Moreover, the fluorescence quenching of neutral DMASBT has been observed above pH 3.7 and the possible reason behind the same has been explained above.

3.4. Quantum chemical calculations

To rationalize the experimental findings and also to locate the TICT state, some semi-empirical quantum chemical calculations have been performed. AM1-SCI calculations [23,24,35–37] have been carried out to determine the optimized geometries of the different conformations of DMASBT to explain their

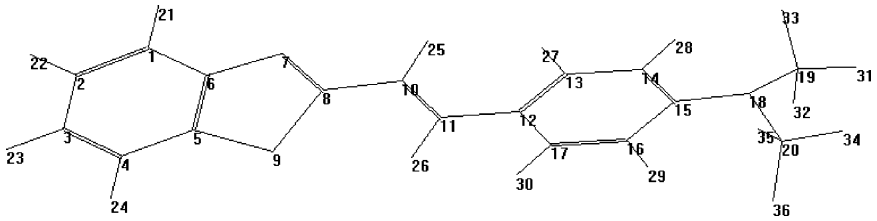

Scheme 3. Optimized geometry of *trans* isomer of DMASBT in the ground state.

properties in the ground and excited states. Scheme 3 represents the optimized geometry of *trans* DMASBT in the ground state. The donor moiety is flexibly linked to the acceptor moiety by the C–N bond. In the Franck-Condon or locally excited (LE) state there is an increase in planarity of the molecule due to the mutual conjugation of nitrogen lone pair orbital and the acceptor π subsystem that may have a fractional internal charge transfer. Rotational motion around C–N bond is described by the torsion angle ϕ (Scheme 1), which is equal to zero when the amino lone pair orbital is perpendicular to the molecular plane of the acceptor subsystem. When the two moieties are orbitally decoupled due to the twisting of the dimethylamino group with respect to the benzene ring of acceptor part ($\phi = 90^\circ$), then full intramolecular charge transfer (ICT) takes place in the excited state. In the ground state the $-N(CH_3)_2$ group in DMASBT shows a pyramidal shape because of the sp^3 hybridization of the nitrogen atom and changes to trigonal planar in the excited state due to a change in hybridization of the nitrogen atom to sp^2 [35]. The experimental findings have already established that DMASBT undergoes TICT in solvents of high polarity. The calculation suggests the requirement of the twisting of the donor group ($-N(CH_3)_2$) perpendicular to the plane of the rest of the molecule for the creation of stable TICT state in polar medium. In this process the overlapping orbitals in the planar geometry get decoupled and as a result of that complete charge transfer takes place.

3.4.1. Locating the TICT state

The TICT state of DMASBT can be well examined through energy evolutions of several excited singlet states as a function of the twist angle (ϕ) between the donor and the acceptor parts of the molecule. Such an examination allows ascertaining the dual fluorescence and can be interpreted in terms of TICT state. This type of analysis has been done for several molecules using a wide range of experimental and theoretical methods [8,35–37,38–41]. Adiabatic energy evolutions of the first four singlet states of DMASBT in relation to the variation of the twist angle ϕ are given in the inset of Fig. 8. AM1-SCI calculations have been used to find out the excited singlet state that is responsible for the increasing TICT emission. On rotating the $-N(CH_3)_2$ moiety in the molecule keeping the rest of the molecule in the *trans* planar form, it can be observed that at an angle of 90°, the S_3 state of the molecule is acquiring a very high dipole moment (12.5 D). The change in the dipole moments of the different singlet states with the variation of the torsion angle (14-15-18-

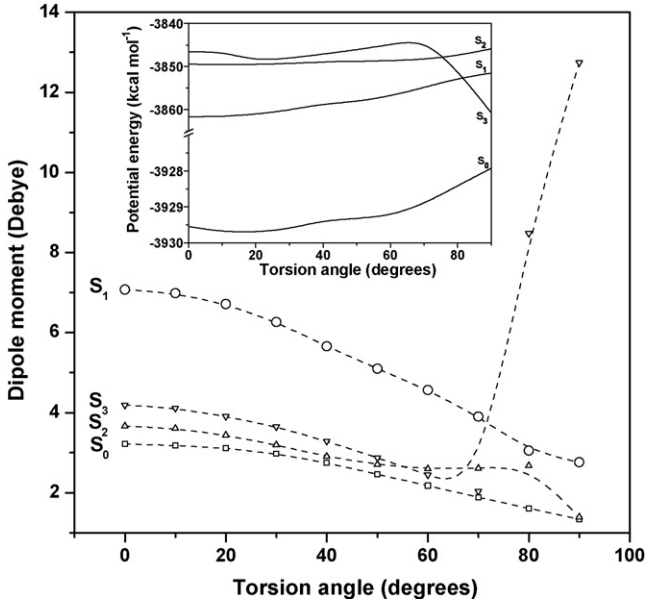

Fig. 8. The variation of dipole moments of DMASBT in first four singlet states with the variation of torsion angle (14-15-18-19, vide Scheme 3). Inset: the variation of energy of DMASBT in water as solvent in first four singlet states with the change of same torsion angle.

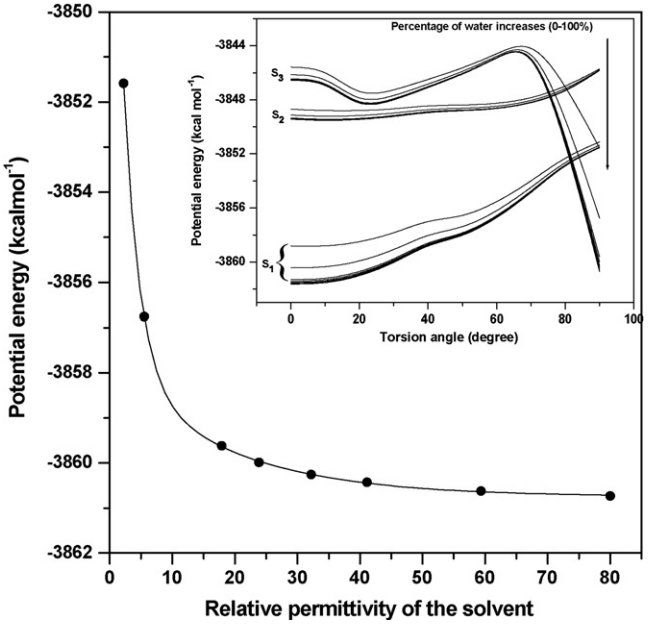

Fig. 9. Plot of change in energy of the S_3 state at the dihedral angle of 90° with changing the relative permittivity of the solvent. Inset: change in energy of first three excited singlet states with changing the torsional angle between the $-N(CH_3)_2$ group and the rest of DMASBT molecule.

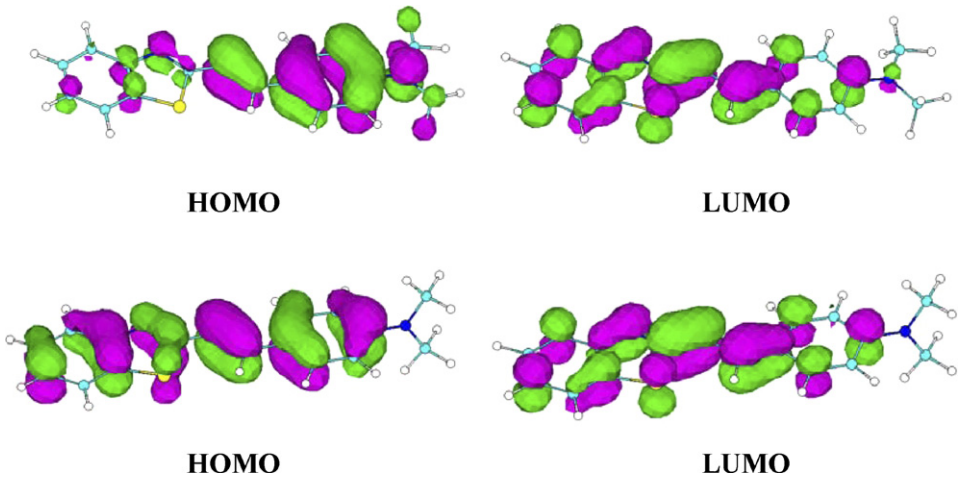

Fig. 10. Frontier molecular orbital (FMO) of DMASBT with the (top) planar (ϕ (14-15-18-19)) = 0°) and (bottom) twisted (ϕ(14-15-8-19)) = 90°) geometries at S_3 state in the gas phase.

19) is illustrated by Fig. 8. Dipole moment of S_3 state increases with increasing the torsion angle, whereas the dipole moments of the other states (S_0, S_1 and S_2) decrease. The remarkable lowering of energy of the S_3 state has been observed at twist angle, $\phi = 90°$, which is consistent with the increase in dipole moment of the S_3 state at the same twist angle. The effect of solvation by each polar solvent results in the lowering of energy of the S_3^{TICT} state even lower than S_1^{LE} as well as S_1^{TICT} states, which makes S_3^{TICT} state responsible for anomalous fluorescence at a critical polarity. These calculations suggest the presence of TICT state and highly Stokes shifted fluorescence in polar solvents and also support the experimental observations [6,12].

On changing the environmental polarity of DMASBT by increasing the percentage of water in dioxane–water mixture, the gradual development of the TICT emission band can be observed. Calculation shows that with increasing relative permittivity (dielectric constant) of the medium, the energy of S_3^{TICT} state of DMASBT gets stabilized remarkably (inset of Fig. 9). The change takes place double-exponentially with increasing polarity of the molecular environment. This indicates a triggering of the TICT process; after the achievement of which the energy of the charge transferred species gets somewhat constant (Fig. 9). It has been observed experimentally that the Stokes shift increases linearly with increasing percentage of water in dioxane–water mixture and ultimately deviates from linearity after a certain concentration of water. The data indicate that any medium with a relative permittivity value ≥ 20 should show TICT emission. The raw data fit well double-exponentially ($\chi^2 = 0.0007$, $R^2 = 0.99997$) confirming the existence of two species, the LE and the TICT with the same contribution [42,43].

Further confirmation of the TICT phenomenon comes from the frontier molecular orbital (FMO) pictures. The nature of the molecular orbitals involved is illustrated by Fig. 10. In the planar geometry, the HOMO and LUMO have considerable delocalization over the whole π system. Both the orbitals are primarily located on the donor and acceptor parts of the molecule. The $S_0 \rightarrow S_3^{LE}$ transition thus occurs only with a fraction of a full electron transfer from the nitrogen atom of $-N(CH_3)_2$ fragment to the remainder of the DMASBT molecule, which results in a calculated dipole moment of ~4.3 D at S_3^{LE} state. At the molecular twist of 90°, π orbitals of $-N(CH_3)_2$ group are completely decoupled from the remaining π orbitals, so that the HOMO → LUMO excitation entails a full electron transfer from the donor to the acceptor. This leads to the formation of the S_3^{TICT} state with a very high dipole moment value of 12.5 D (experimentally found value is 11.26 D), which on stabilization due to solvation with a solvent of high polarity becomes responsible for the highly Stokes shifted fluorescence. In the gas phase, the energies of TICT states are greater than the respective planar S_1 and S_2 states, whereas the energy of S_3^{TICT} state is lower than the S_3 planar state. The dipole moment of only the S_3^{TICT} state among the first four singlet states is greater than the respective planar state. This dipole moment is large enough relative to the dipole moments of the remaining states to locate the TICT state by the dielectric continuum estimation in polar solvents [44].

4. Conclusions

DMASBT has been found to be a very sensitive TICT molecule in polar solvents. The results obtained from AM1-SCI quantum chemical calculations are in good agreement with the experimental observations. The quantum chemical calculations show that the S_3 state of the molecule gets stabilized in polar solvents due to the development of high dipole moment as a consequence of the twist ($\phi = 90°$) in the $-N(CH_3)_2$ moiety with respect to the rest of the molecule. Behavior of TICT fluorescence in a mixed solvent with hydrogen-bonding propensity could nicely be explained by the potential energy calculations of the TICT states considering the effect of dielectric constants of mixed solvents (dioxane and water) of varying compositions. Based on multiparametric regression analysis, it appears that the ground state stabilization is mainly determined by the dipolar interactions and hydrogen-bond acceptor ability of solvents. But, all the three parameters, π^*, α, and β, contribute to the stabilization of the excited state. However, dipolar interactions provide the major contributions to the stability of ground as well

as excited states. This contribution is greater in the excited state than that in the ground state. High fluorescence quantum yields in polar viscous medium may be due to the restriction of rotational motions of the molecule. Fluorescence quantum yields are low in most of the solvents due to the high possibility of non-radiative processes. In addition to the change in fluorescence quantum yields, Stokes shifts are also substantially changed with increasing the polarity and viscosity of the medium. In this regard DMASBT can be a potential candidate not only due its high sensitivity towards polarity and pH, but also due its high sensitivity towards viscosity, because in addition to change in polarity and pH, viscosity change of biological systems may also occur simultaneously. Therefore, the present study provides a molecular probe as a microsensor to study biological functions as well as biomimicking systems. The decrease of TICT fluorescence of DMASBT with increasing pH above 3.7 suggests that water molecules become efficient for hydrogen-bonding interactions only above this pH. This prompts us to suggest that DMASBT may be used as a sensor to sense the hydrogen-bonding efficiency of the medium. Further attempts are being taken to know better about the molecule in confined *in vitro* biomimicking environments.

Acknowledgements

Financial support and facilities provided by Birla Institute of Technology and Science, Pilani, India are gratefully acknowledged. The authors also extend their acknowledgement to Professor Nitin Chattopadhyay of Department of Chemistry, Jadavpur University, Calcutta, India for allowing them to use the HyperChem software. One of the authors (PP) gratefully acknowledges the financial support from the DST, Govt. of India for the project number SR/FTP/CS-114/2005 under the SERC Fast Track scheme. The authors gratefully acknowledge one of the reviewers for his critical comments on the present manuscript that helped them to improve the report substantially.

References

[1] E.G. Moore, P.V. Bernhardt, A. Fürstenberg, M.J. Riley, E. Vauthey, J. Phys. Chem. A 109 (2005) 11715–11723.
[2] A. Zehnacker, F. Lahmani, J. Phys. Chem. A 104 (2000) 1377–1387.
[3] M. Maus, Photoinduced Intramolecular Charge Transfer in Donor–Acceptor Biaryls and Resulting Applicational Aspects Regarding Fluorescent Probes and Solar Energy Conversion, Universal Publishers, USA, 1998.
[4] M. Sadownik, P. Bojarski, Chem. Phys. Lett. 396 (2004) 293–297.
[5] K.A. Zachariasse, T. von der Haar, A. Hebecker, U. Leinhos, W. Kuhnle, Pure Appl. Chem. 65 (1993) 1745–1750.
[6] A.E. Nikolaev, G. Myszkiewicz, G. Berden, W.L. Meerts, J.F. Pfanstiel, D.W. Pratt, J. Chem. Phys. 122 (2005), 084309-1-10.
[7] K. Rotkiewicz, K.H. Grellmann, Grabowski, Z. R. Chem. Phys. Lett. 19 (1973) 315–318.
[8] Z.R. Grabowski, K. Rotkiewicz, A. Siemiarczuk, D.J. Cowley, W. Baumann, Nouv. J. Chim. 3 (1979) 443–454.
[9] V. Bonacic-Koutecky, P. Bruckman, P. Hiberty, J. Koukecky, C. Leforestier, L. Salem, Angew. Chem. 87 (1975) 599–601.
[10] M.C. Cuquerella, M.A. Miranda, F. Bosca, J. Phys. Chem. A 110 (2006) 2607–2612.
[11] S.I. Druzhinin, N.P. Ernsting, S.A. Kovalenko, L.P. Lustres, T.A. Senyushkina, K.A. Zachariasse, J. Phys. Chem. A 110 (2006) 2955–2969.
[12] Z.R. Grabowski, K. Rotkiewicz, W. Rettig, Chem. Rev. 103 (2003) 3899–4032.
[13] Z.R. Grabowski, J. Dobkowski, Pure Appl. Chem. 55 (1983) 245–252.
[14] T.A. Fayed, S.S. Ali, Spectrosc. Lett. 36 (2003) 375–386.
[15] J. Dey, E.L. Roberts, I.M. Warner, J. Phys. Chem. A 102 (1998) 301–305.
[16] M.A. Haidekker, T.P. Brady, D. Lichlyter, E.A. Theodorakis, Bioorg. Chem. 33 (2005) 415–425.
[17] J. Dey, I.M. Warner, J. Phys. Chem. A 101 (1997) 4872–4878.
[18] M.J. Kamlet, J.-L.M. Abboud, M.H. Abraham, R.W. Taft, J. Org. Chem. 48 (1983) 2877–2887.
[19] S.K. Saha, S.K. Dogra, J. Mol. Struct. 470 (1998) 301–311.
[20] P. Purkayastha, S.C. Bera, N. Chattopadhyay, J. Mol. Liq. 88 (2000) 33–42.
[21] S.K. Saha, S. Pandey, S.K. Dogra, Indian J. Chem. 34A (1995) 771–777.
[22] M.J.S. Dewar, E.G. Zoebisch, E.F. Healy, J.J.P. Stewart, J. Am. Chem. Soc. 107 (1985) 3902;
M.J.S. Dewar, K.M. Dieter, J. Am. Chem. Soc. 108 (1986) 8075–8086;
J.J.P. Stewart, J. Comput. -Aided Mol. Des. 4 (1990) 1–105.
[23] J.J.P. Stewart, J. Comput. Chem. 10 (1989) 221–264, 209–220.
[24] C.J.F. Bottcher, Theory of Electronic Polarization, vol. 1, Elsevier, Amsterdam, 1983.
[25] A. Mallick, S. Maiti, B. Haldar, P. Purkayastha, N. Chattopadhyay, Chem. Phys. Lett. 371 (2003) 688–693.
[26] F. Cichos, A. Willert, U. Rempel, C.V. Borczyskowski, J. Phys. Chem. A 101 (1997) 8179–8185.
[27] Z.R. Grabowski, K. Rotkiewicz, A. Siemiarczuk, J. Lumin. 18/19 (1979) 420–424.
[28] E.M. Kosower, H. Dodiuk, K. Tanizawa, M. Ottolenghi, N. Orbach, J. Am. Chem. Soc. 97 (1975) 2167–2178.
[29] Y.L. Khmelnitsky, V.V. Mozhaev, A.V. Bellova, M.V. Sergeeva, K. Martinek, Eur. J. Biochem. 198 (1991) 31–41.
[30] M. Ravi, A. Samanta, T.P. Radhakrishnan, J. Phys. Chem. 98 (1994) 9133–9136.
[31] P. Avouris, W.M. Gelbert, M.A. El-Sayed, Chem. Rev. 77 (1977) 793–833.
[32] R. Das, D. Guha, S. Mitra, S. Kar, S. Lahiri, S. Mukherjee, J. Phys. Chem. A 101 (1997) 4042–4047.
[33] L.E. Cramer, K.G. Spears, J. Am. Chem. Soc. 100 (1978) 221–227.
[34] S. Swaminathan, S.K. Dogra, J. Am. Chem. Soc. 105 (1983) 6223–6228.
[35] A.-D. Gorse, M. Pesquer, J. Phys. Chem. 99 (1995) 4039–4049.
[36] P. Purkayastha, N. Chattopadhyay, Phys. Chem. Chem. Phys. 2 (2000) 203–210.
[37] P. Purkayastha, N. Chattopadhyay, Int. J. Mol. Sci. 4 (2003) 335–361.
[38] S. Kato, Y. Amatatsu, J. Chem. Phys. 92 (1990) 7241–7257.
[39] J. Lipinski, H. Chojnacki, Z.R. Grabowski, K. Rotkiewicz, Chem. Phys. Lett. 70 (1980) 449–453.
[40] S. Marguet, J.C. Mialocq, P. Millie, G. Berthier, F. Momicchioli, Chem. Phys. 160 (1992) 265–279.
[41] J.P. LaFemina, C.B. Duke, A. Paton, J. Chem. Phys. 87 (1987) 2151–2157.
[42] S. Kundu, N. Chattopadhyay, J. Mol. Struct. 344 (1995) 151–155.
[43] J. Otani, H. Yamamoto, M. Fukuda, K. Kodama, J. Lumin. 104 (2003) 273–281.
[44] Y. Amamatsu, Theor. Chem. Acc. 103 (2000) 445–450.